

# Characterisation and performance of a Terfenol-D coated femtosecond laser inscribed optical fibre Bragg sensor with a laser ablated microslot for the detection of static magnetic fields

G.N. Smith,<sup>1,\*</sup> T. Allsop,<sup>1</sup> K. Kalli,<sup>2</sup> C. Koutsides,<sup>2</sup> R. Neal,<sup>3</sup> K. Sugden,<sup>1</sup>  
P. Culverhouse,<sup>3</sup> and I. Bennion<sup>1</sup>

<sup>1</sup>Photonics Research Group, Aston University, Aston Triangle, Birmingham, B4 7ET, United Kingdom

<sup>2</sup>Nanophotonics Research Laboratory, Cyprus University of Technology, Department of Electrical Engineering and Information Technology, 33 Saripolou Street, Lemessos 3036, Cyprus

<sup>3</sup>School of Computing, Communications and Electronics, Faculty of Technology, University of Plymouth, Plymouth PL4 8AA, UK

\*smithgn@aston.ac.uk

**Abstract:** We present a novel device for the characterisation of static magnetic fields through monitoring wavelength shifts of femtosecond inscribed fibre Bragg grating and micromachined slot, coated with Terfenol-D. The device was sensitive to static magnetic fields and can be used as a vectorial sensor for the detection of magnetic fields as low as 0.046 mT with a resolution of  $\pm 0.3$  mT in transmission and  $\pm 0.7$  mT in reflection. The use of a femtosecond laser to both inscribe the FBGs and micromachine the slot in a single stage prior to coating the device significantly simplifies the fabrication.

© 2010 Optical Society of America

**OCIS codes:** (060.3735) Fiber Bragg gratings; (060.2370) Fiber optics sensors; (350.3390) Other areas of optics: Laser materials processing.

---

## References and links

1. A. E. Clark, *Ferromagnetic Materials*, (North Holland, 1986), Vol. 1.
2. A. Yariv, and H. V. Winsor, "Proposal for detection of magnetic fields through magnetostrictive perturbation of optical fibers," *Opt. Lett.* **5**(3), 87–89 (1980).
3. J. P. Willson, and R. E. Jones, "Magnetostrictive fiber-optic sensor system for detecting dc magnetic fields," *Opt. Lett.* **8**(6), 333–335 (1983).
4. R. Rajini-Kumar, M. Suesser, K. G. Narayankhedkar, G. Krieg, and M. D. Atrey, "Performance evaluation of metal-coated fiber Bragg grating sensors for sensing cryogenic temperature," *Cryogenics* **48**(3-4), 142–147 (2008).
5. F. Bucholtz, C. A. Villarruel, C. K. Kirkendall, D. M. Dagenais, J. A. McVicker, A. R. Davis, S. S. Patrick, K. P. Koo, and A. Dandridge, "8 element array of 3-axis fiber optic magnetometers for undersea applications," in *Tenth International Conference on Optical Fibre Sensors*, B. Culshaw and J. D. C. Jones, eds. (Spie - Int Soc Optical Engineering, Bellingham, 1994), pp. 36–39.
6. L. Fabiny, S. T. Vohra, and F. Bucholtz, "Multiplexed Low-Frequency Electric and Magnetic Field Fiber Optic Sensors," *Opt. Fiber Technol.* **2**(1), 106–113 (1996).
7. L. Sun, S. Jiang, and J. R. Marciante, "All-fiber optical magnetic-field sensor based on Faraday rotation in highly terbium-doped fiber," *Opt. Express* **18**(6), 5407–5412 (2010).
8. M. H. Kim, K. S. Lee, and S. H. Lim, "Magnetostriction measurements of metallic glass ribbon by fiber-optic Mach-Zehnder interferometry," *J. Magn. Magn. Mater.* **191**(1-2), 107–112 (1999).
9. M. Sedlar, V. Matejec, and I. Paulicka, "Optical fibre magnetic field sensors using ceramic magnetostrictive jackets," *Sens. Actuators A Phys.* **84**(3), 297–302 (2000).
10. W. Xin, C. Shuying, D. Zhigang, W. Xiaoyang, S. Changhai, and C. Jianping, "Experimental Study of Some Key Issues on Fiber-Optic Interferometric Sensors Detecting Weak Magnetic Field," *Sensors J. IEEE* **8**(7), 1173–1179 (2008).
11. P. D. Dinev, "A two-dimensional remote fibre-optic magnetic field and current sensor," *Meas. Sci. Technol.* **7**(9), 1233–1237 (1996).
12. U. Holm, H. Sohlstrom, and T. Brogardh, "Measurement system for magneto-optic sensor materials," *J. Phys. E Sci. Instrum.* **17**(10), 885–889 (1984).

13. M. H. Yang, J. X. Dai, C. M. Zhou, and D. S. Jiang, "Optical fiber magnetic field sensors with TbDyFe magnetostrictive thin films as sensing materials," *Opt. Express* **17**(23), 20777–20782 (2009).
14. G. Vértesy, A. Gasparics, and Z. Vértesy, "Improving the sensitivity of Fluxset magnetometer by processing of the sensor core," *J. Magn. Magn. Mater.* **196–197**, 333–334 (1999).
15. M. V. Dubov, M. Amos, K. Igor, and B. Ian, "Point by point FBG inscription by a focused NIR femtosecond laser," in *Technical Digest (CD)* (Optical Society of America, 2004), CMY6.
16. T. Geernaert, K. Kalli, C. Koutsides, M. Komodromos, T. Nasilowski, W. Urbanczyk, J. Wojcik, F. Berghmans, and H. Thienpont, "Point-by-point fiber Bragg grating inscription in free-standing step-index and photonic crystal fibers using near-IR femtosecond laser," *Opt. Lett.* **35**(10), 1647–1649 (2010).
17. G. Ghosh, M. Endo, and T. Iwasaki, "Temperature-dependent Sellmeier coefficients and chromatic dispersions for some optical-fiber classes," *J. Lightwave Technol.* **12**(8), 1338–1342 (1994).
18. C. C. Lai, W. Y. Lee, and W. S. Wang, "Gamma radiation effect on the fiber Fabry-Perot interference sensor," *IEEE Photon. Technol. Lett.* **15**(8), 1132–1134 (2003).
19. A. Othonos, and K. Kalli, *Fiber Bragg Gratings: fundamentals and applications in telecommunications and sensing* (Artech House Optoelectronics Library, 1999), p. 422.
20. D. Davino, C. Visone, C. Ambrosino, S. Campopiano, A. Cusano, and A. Cutolo, "Compensation of hysteresis in magnetic field sensors employing Fiber Bragg Grating and magneto-elastic materials," *Sens. Actuators A Phys.* **147**(1), 127–136 (2008).

## 1. Introduction

Magnetic sensors are widely used to control and analyse a wide range of devices and natural and manmade processes, examples of which are linear and rotary position sensing, current sensing, the measurement of geophysical anomalies, various physiological functions, metal defects. Using a range of optical detection methods, such as interferometry, Faraday rotation and cantilever arrangements covering fields from 1nT to ~1T. Here we use Terfenol-D, as part of a fibre Bragg grating sensor device, which in the presence of magnetic fields changes dimensions. The physical effect, in this case, is giant magnetostriction which changes the physical dimensions in the presence of relatively small magnetic fields. The alloying of Dysprosium, Dy, and Terbium Tb; DyFe<sub>2</sub>, and TbFe<sub>2</sub> has the form Tb<sub>x</sub>Dy<sub>1-x</sub>Fe<sub>2</sub> (where typically x = 0.3) gives the highest known magnetostrictive compound exhibiting approximately 2,000 microstrains in a field of 2 kOe (160 kA/m) at room temperature [1]. When operating below the Curie temperature, as in this experiment, the relationship remains linearly proportional between the strain and magnetic field strength.

The concept of integrating magnetostriction and fibre strain sensors was first proposed to detect small magnetic fields in 1980 [2] and achieved in 1983 [3]. However, the sensitivity of these sensors improved with the use of FBGs adding to the other advantages of multiplexing, cost, immunity to EM interference and compact spatial requirements, and ability to remotely work in hostile conditions [4–6]. Prior work has been concentrated on three techniques for combining the magnetostrictive material and the fibre sensor; bonding, coating and doping [7–9]. The mechanisms for detection have been focused on interferometer set-ups [8–10] although other techniques such as using Faraday rotation and cantilevers have been reported [7,11,12]. Most reported studies were conducted using high frequency magnetic fields or by using mumetal shields leading to practical application issues for detecting either slowly varying or static magnetic fields.

In this paper we present a novel device for the characterisation of static magnetic fields using a femtosecond inscribed fibre Bragg grating (FBG) with a femtosecond micromachined slot coated with Terfenol-D. The device was shown to have sensitivity to magnetic fields of 0.3 pmmT<sup>-1</sup> in transmission and 0.2 pmmT<sup>-1</sup> and 0.1 pmmT<sup>-1</sup> for different polarisation states in reflection and a thermal sensitivity of 114pm°C<sup>-1</sup>. These results show the device has the potential for use as a vectoral sensor for the detection of magnetic fields as low as 0.046 mT with a resolution of ± 0.3mT in transmission and ± 0.7mT in reflection. An important feature of this work is that it significantly simplifies the fabrication of the sensing devices by using one laser to create the FBG and micromachined slot.

It has been shown that the sensitivity of magnetostrictive fibre sensors is increased by removing the cladding through chemical etching thus reducing the ratio between the fibre and

Terfenol-D coating [13]. However, the use of chemical processing using HF is slow and has numerous related health and safety issues. Instead we use a single femtosecond laser processing to both inscribe a grating and micro-machine a slot. The slot is designed to both increase sensitivity, through a relative increase in the ratio of Terfenol-D to fibre cladding, and break the radial symmetry leading to the sensors potential vectoral capability. We then use sputtering as the method of attaching the Terfenol-D to the fibre as this had been shown to give the most sensitive detection and avoided a number of flaws with the other techniques, i.e. low sensitivity with the Faraday effect and the inefficiency of bonding the fibre to a strip [14]. During sputtering the micromachined slot is back filled with the Terfenol-D creating a robust monolithic structure.

The resulting sensors demonstrate high sensitivity to weak static magnetic fields with the use of one sensor device with a two step processing with cheap components and standard components. The results also show sensitivity to the magnetic field direction which has previously not been demonstrated by comparable approaches.

## 2. Fabrication and characterisation

The sensor was made using a three step process. First a low insertion loss fibre Bragg grating, FBG, was inscribed point by point [15,16] in Corning single mode fibre-28 using a femtosecond laser (a High Q femtoREGEN laser operating at 1035nm, with pulse duration of 300fs, 1kHz pulse repetition rate with the pulse energy being controlled by a variable attenuator.). A Mitutoyo x50 NIR lens was used as it provides a long working distance with a moderate NA thus generating a small and highly accurate focal spot that the structures written required. The accurate nature of the spot through the sample due to the large NA and working distance are critical to the direct write nature of the work. The fibre was suspended between fibre mounts on a high precision Aerotech air bearing 2D translation stage, Fig. 1a. Once the focal spot of the laser beam had been aligned the stage were then translated at a velocity of  $1.07\text{mms}^{-1}$  creating a 2nd order grating with a pitch of  $1.07\mu\text{m}$  over 30mm in the centre of the fibre core in order to be resonant at approximately 1550nm. The grating inscribed had an effective optical strength of 1dB as measured in transmission, typical of femtosecond inscribed low loss gratings written in this manner.

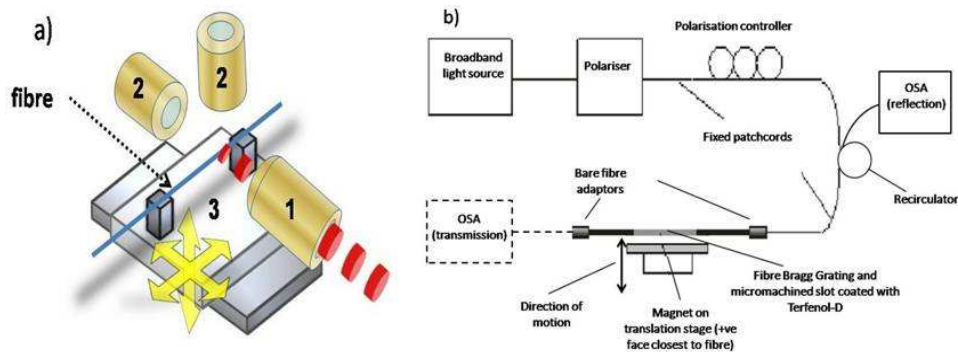


Fig. 1. a) Schematic of the inscription technique, 1 indicates the position of the 50x objective lens, 2 the vision optics for alignment and 3 the stages used for motion, b) Schematic of the characterisation apparatus for transmission and reflection for one of the vectors' characterisation (the mount being altered for the perpendicular vectors).

The second step was to micromachine a slot, using the same laser and set-up, into the cladding of the fibre directly in line with the region of the grating. The alignment was achieved by aligning to the core of the fibre then stepping the fibre jig  $65\mu\text{m}$  away from the focussing lens so the plasma is at the air cladding boundary. The slot was then created using multiple scans of a set area in the direction of the fibre axis with pulse energy of  $10\mu\text{J}$  until the

plasma diminished. Typically 10 passes in both directions were made at each depth. The fibre was subsequently translated progressively towards the fibre core in 10 $\mu$ m increments and the scanning was repeated. During the machining the fibre grating response was monitored using a light source and optical spectrum analyser. This enabled the ablated slot depth to be controlled and repeatable. Slot lengths up to 30mm long, 15 $\mu$ m wide and with a depth of 20 $\mu$ m were fabricated exactly overlapping the region where the FBG was located. The third step was to uniformly coat the fibre, including back filling the groove section, with the alloy Terfenol-D using sputter machine and mask. This was achieved by mounting the fibre device in a coating jig and rotating it at 60 revs/min, in a vacuum level better than 10<sup>-6</sup> mbar, Argon pressure at 5 $\mu$ m of Hg, using an RF Power level of 200 Watts. The coating was carried out in two 30 minute long sessions chosen to minimise overheating of the device resulting in a total coating thickness of 1 $\mu$ m. The relative dimensions of the Terfenol-D monolith to cladding changes the sensitivity of the device, with greater sensitivity achieved with larger monolith. This was an initial thickness chosen to ensure complete backfill of the monolith. The final device design is shown in the schematic in Fig. 2.

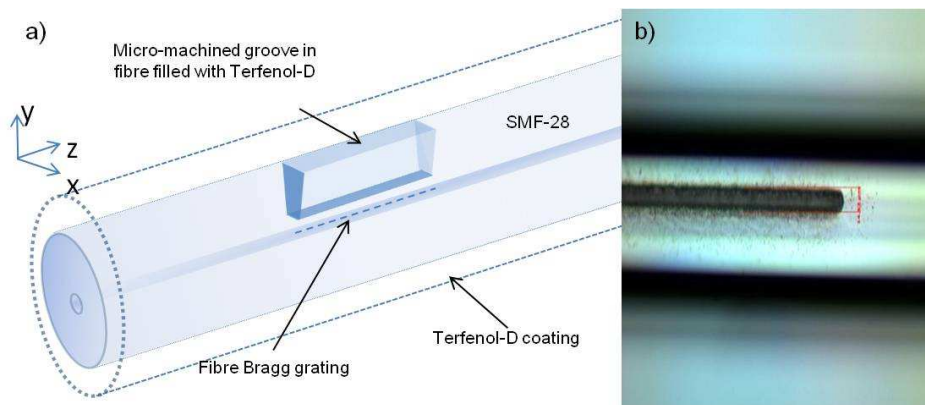


Fig. 2. a) Schematic of the geometry of the magnetic optical fibre sensor device with smf28 with femtosecond inscribed FBG in the core and micromachined slot which is then back filled and coated with Terfenol-D, b) Microscope image of the slot in the Corning single mode fibre-28 prior to being filled and coated.

The characterisation of the sensor was carried out through interrogation of both transmission and reflection spectra under the variation of magnetic field strength. The schematic in Fig. 1b shows the two set-ups used. The device was also characterised for its thermal sensitivity using a peltier. The fibre devices are characterised with a broadband light source (ELED) which is passed through a polariser (PAT8000B) and a polarisation controller and a coupler before illumination of the sample, with the transmission/reflection spectra being monitored using an optical spectrum analyser (Agilent 86142B with resolution bandwidth of 0.06nm).

The static magnetic field was created using a permanent magnet mounted on a 3D translation stage which was then translated in micron scale increments towards and away from the fibre in the 3 directions indicated in Fig. 2 (x, y, z). The spectra were captured at each position and subsequently the centroid of each resonance was calculated and analysed. Since the grating shape is constant and relatively broadband it is possible using centroid peak fitting to achieve a measurement resolution greater than the resolution bandwidth of the OSA. The magnets used were calibrated with a Phillips & Harris magnetic flux density meter that has a calibrated accuracy to within  $\pm 0.1$  mT. The spatial distribution of magnetic flux density generated by the magnets was determined and the results used to infer the field strength at a given separation distance between the sensor and the magnets. A static field was used as it

created no temperature increase of the surroundings as was found to be the case when a DC current source was used with a coil in initial experimentation.

### 3. Experimental results

The polarisation dependence of these devices was investigated due to the asymmetric geometry of the sensor itself. A small variation was observed in both the transmission and reflection spectra, an example in reflection is shown in Fig. 3 with the spectral sensitivity shown in Fig. 4.

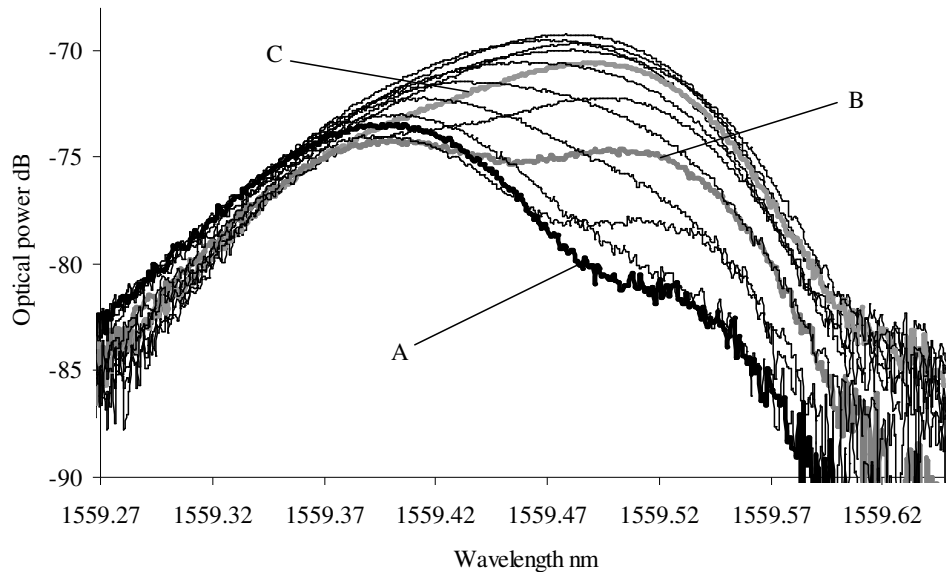


Fig. 3. Polarisation variation in the reflective spectral response of the sensor (coating thickness  $1\mu\text{m}$ , length of groove and Bragg grating  $2\text{cm}$ ).

Although the sensors were made in standard fibre rather than polarisation maintaining fibre the polarisation dependence was still measured in a relative context. Figure 3 shows a typical set of reflection spectra of the complete sensor as a function of varying the polarisation. The figure shows two clear states A and C and a range of intermediate states with B being a good example. Polarisation state A showed little sensitivity and is believed to be the state perpendicular to that of the monolith. State C showed the greatest sensitivity and is believed to be orthogonal to A and thus in line with the monolith structure. State B is believed to be the resultant of states A and C. The dB drop shows that it is likely to be at slightly less than  $45^\circ$  from state C, however, this is expected as the slot and subsequent monolith has physical volume.

Figure 4 shows how the calculated centroid wavelength and the optical strength of the device measured in reflection changes as the polarisation does. The plot demonstrates the degree of polarisation dependence on the response of the device showing a  $90^\circ$  variation between maximum and minimum as would be expected from a device with a slot in one axis.

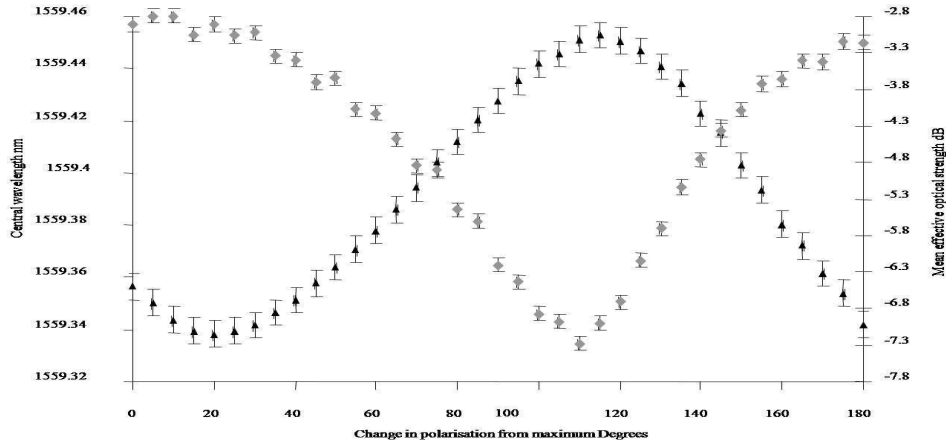


Fig. 4. The variation in the centroid wavelength and effective optical strength of the reflective spectra as a function of changing polarisation.

The effect of magnetic field strength on the different polarisation states of the sensor in reflective spectrum operation was investigated using a device with a coating thickness of  $1\mu\text{m}$ , and groove length and FBG length of  $2\text{cm}$ . The polarisation state believed to be in line with the monolith (C) and the intermediate polarisation state (B) showed magnetic field strength sensitivity and the other (A) showed little response. The polarisation states B and C yielded sensitivities of  $0.1\text{ pmmT}^{-1}$  and  $0.2\text{ pmmT}^{-1}$  respectively with obvious strength change, see Figs. 5. The minimum detectable field was around  $110\text{mT}$ .

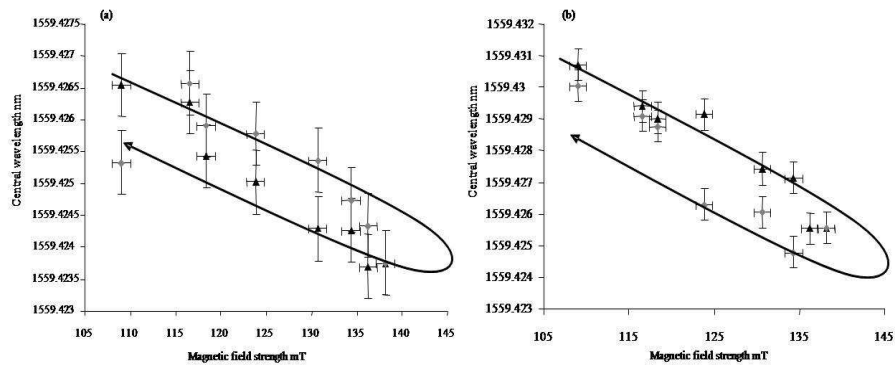


Fig. 5. The spectral response in reflection of the polarisation states of the optical sensor as a function of magnetic field strength, (a) for polarisation state B, (b) for polarisation state C for increasing field strength ( $\blacktriangle$ ) and decreasing field strength ( $\blacklozenge$ ).

Figure 6 shows measurements taken in transmission using a device which has a total groove length of  $3\text{cm}$  and a Bragg grating of  $3\text{cm}$ . The resulting sensitivities are  $0.5\text{pmmT}^{-1}$  and  $0.3\text{pmmT}^{-1}$ , using a magnet in orientation shown in Fig. 1b. The increase in sensitivity of the device in transmission is due to the device length being longer than when examined in reflection after a breakage unrelated to its manufacture during additional testing had left almost all but not quite the complete initial device length intact. The sensitivity recorded was  $\Delta\lambda/\Delta B \sim 0.3\text{ pmmT}^{-1}$  with limited hysteresis in a range between  $22$  and  $32\text{ mT}$ .

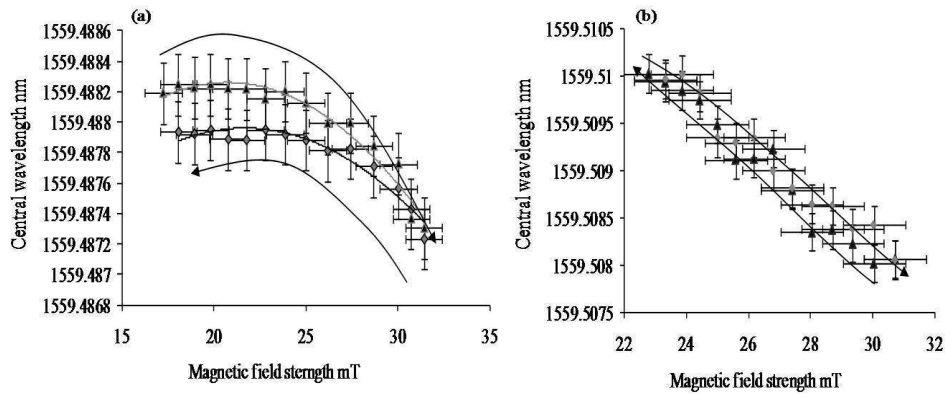


Fig. 6. The spectral characteristics of the device in transmission of the polarisation states of the optical sensor (coating thickness  $1\mu\text{m}$ , length of groove and Bragg grating  $3\text{cm}$ ) as a function of magnetic field strength, (a) for polarisation state A, (b) for polarisation state C for increasing field strength ( $\blacktriangle$ ) and decreasing field strength ( $\blacklozenge$ ).

The thermal sensitivity of the device was calculated experimentally by placing the fibre in a calibrated peltier. Care was taken to lay the fibre as straight as possible as to avoid any extraneous polarisation effects. The reflected spectra were recorded at each temperature, once stabilised, at  $10^\circ\text{C}$  intervals from  $20$  to  $80^\circ\text{C}$  its thermal response was found to be  $11.4\text{pm}^\circ\text{C}^{-1}$ . The results are shown in Fig. 7. Although significant this is within the common range for thermal sensitivity for FBG in smf28 and was negated in the magnetic sensitivity experiments by maintaining a constant room temperature. We are currently developing a temperature compensated version of the device.

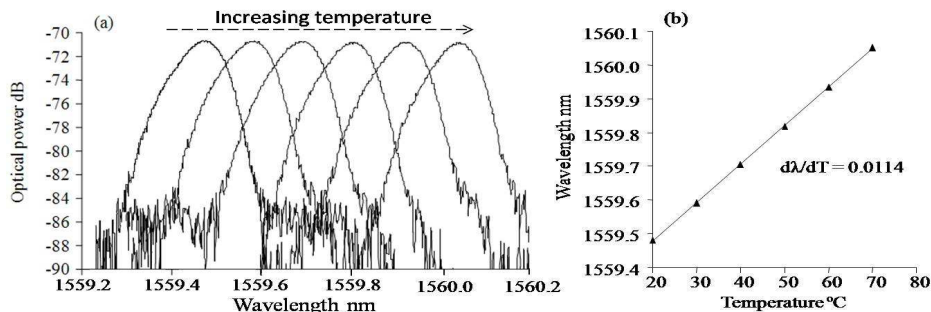


Fig. 7. The spectral response of the optical sensor as a function of temperature (a) the reflective spectra, (b) spectral sensitivity

#### 4. Analysis of experimental results

The device's spectral characteristics, in an insulated and temperature controlled environment, were also investigated to understand the stability and resolution of this approach. Looking specifically at the standard deviation in wavelength of the in response in the reported device, a variation of  $\pm 0.014\text{pm}$  was seen over a time period of 5 minutes, this is thought to be due to the small amount of temperature variation within the peltier device. For standard FBGs the thermal response is typical  $1\text{pm}$  for  $0.1^\circ\text{C}$  change in temperature. If the assumption is correct, then the minimum sensitivity threshold for the temperature stabilised  $3\text{cm}$  transmission sensor device with sensitivity  $0.3\text{pmmT}^{-1}$ , is found to be  $0.047\text{mT}$ . This is greater than the cross-sensitivity between the magnetic and thermal response of the sensor device, which when

calculated using the experimental data and material constants from references [1,17–19] was estimated to be  $\sim 3 \times 10^{-3} \text{ pm}^\circ\text{C}^{-1}\text{T}^{-1}$ .

Fitting a linear response to the data of the 3 cm long fibre sensor a residual average error of  $\pm 0.12 \text{ pm}$  was seen. This leads to a resolution limit of  $\pm 0.3 \text{ mT}$  in a magnetic field strength of  $\sim 20 \text{ mT}$ . For the 2 cm fibre sensor, working in reflection, a resolution limit of  $\pm 0.7 \text{ mT}$  in magnetic field strengths of  $\sim 110 \text{ mT}$  was observed.

Although the sensor device has characteristic hysteresis it has been shown that this may be accounted for with algorithms which compensate for the rate independent memory effects. This has been demonstrated to be effective for other FBG magnetic strain sensors in improving the accuracy and linearity range of the device [20]. This type of algorithm could be applied to track the global performance of the device making it more accurate and reliable.

The data presented demonstrates that the response of the sensor is very much dependent upon its separation distance, i.e. field strength, and orientation relative to the magnetic field. This accounts for the differences in sensitivities between the various experiments and shows the expected behaviours of the designed asymmetric sensor geometry. When tested the device showed varying sensitivity to vectoral variation in magnetic flux density (through translation of the magnet in x, y and z), however, as the fibre was completely coated in order to ensure complete back fill the exact orientation of the monolith relative to the motion of the stages was unknown and as such could not be calibrated fully and is a source of current further investigation.

Whilst this is not as sensitive as some reported results elsewhere, where minimum detectable magnetic fields of  $0.10 \text{ nT Hz}^{-1/2}$  and sensitivities of up to  $1.08 \text{ pmmT}^{-1}$  [10,13] were presented, however, the asymmetry of the device enables it to be sensitive to the direction of the magnetic field which is highly novel in the case of fibre sensors. The device also does not rely on high frequency AC magnetic fields, multilayer coatings, mumetals or expensive Fabry-Perot filters to work. The laser fabrication process and subsequent filling of the machined slot means it is also mechanically stronger than the chemically etched fibres and the devices could be easily multiplexed, which with other interrogation systems can prove problematic, with gratings at different wavelengths for distributed monitoring. The results are more sensitive than the Faraday rotation devices which have similar levels of simplicity in their optical configuration which have been shown to measure fields from 0.02 to 3.2T [7].

## 5. Conclusion

A novel static magnetic field sensor based on single layer magnetostrictive film of Terfenol-D sputtered onto a single mode fibre that had a femtosecond inscribed FBG and slot micromachined into it is presented in this work. It has demonstrated a minimum detection limit of  $0.047 \text{ mT}$  and a sensitivity of  $0.3 \text{ pmmT}^{-1}$  in transmission with a resolution limit of  $\pm 0.3 \text{ mT}$  in a magnetic field strength of  $\sim 20 \text{ mT}$ . The sensor device clearly demonstrates potential for vectoral field sensing capability. The simplicity of the optical configuration and results show the potential for this technique to be applied to a range of fields due to its small sensor size and ability to be remotely interrogated. This demonstrates the potential for vectoral magnetic field sensing with high sensitivity and large scope for flexibility.

## Acknowledgments

The authors would like to acknowledge financial support for this work from the EU project PHOSFOS “Photonic Skins for optical fibre sensors”.